Generation of divergence-free Bessel-Gauss beam from an axicon doublet for km-long collimated laser

Sirawit Boonsit[1,2], Panuwat Srisamran[1,2], Pruet Kalasuwan[1,2], Paphavee van Dommelen[1,2] and Chalongrat Daengngam*

[1]Department of Physics, Faculty of Science, Prince of Sonkla University, Songkhla, Thailand, 90110
[2]Thailand Center of Excellence in Physics, Commission on Higher Education, Bangkok, Thailand, 10400
*chalongrat.d@psu.ac.th

Abstract:
A well-collimated intensity profile at long distance has long been a desired laser property crucial for many potential applications. Extending a non-diverging range for ordinary laser beyond kilometers scale would permit superior performance for optical technologies, including LIDAR, or free-space communication. In this paper, we propose a facile but powerful technique to generate a long-range non-diverging beam from a cemented axicon doublet structure. The system is all solid-state with optical design parameters based on current technological availability. A compound axicon here is expected to provide sufficiently low beam converging beyond the limit of a single axicon. The resulting beam profile is regarded as Bessel-Gauss with inward radial wave component that compensates diffraction of a normal Gaussian mode profile. A numerical simulation was performed to verify for km-long laser propagation domain, accomplished by using Electromagnetic Wave Beam Envelop interface in COMSOL Multiphysics®, which allows finite element simulation for wave optics in an ultra large domain without spending excessive resources. It was found that, with an input beam waist of only 25 mm, an axicon doublet at optimal parameters can generate a Bessel-Gauss beam with divergent-free range of at least 2 km.

Keywords: divergence-free beam, Bessel-Gauss beam, axicon doublet,

1. Introduction

Thanks to incessant research and development, laser science and technology have advanced significantly since the first invention in 1960, which enable numerous potential applications, such as standoff Raman detections for explosive or hazard chemicals [1], light detection and ranging (LIDAR) [2], hyperspectral imaging [3], defensive laser system [4], ultrahigh bit rate free-space communication [5], or even an envisaged laser propulsion of an spacecraft for deep space exploration [6]. It is well aware that the performance of those aforementioned applications strictly relies on the quality and intensity profile of a laser beam at remote distance. However, as a wave, a laser beam possesses an unfavorable drawback of beam divergence caused by diffraction, which rapidly reduces laser intensity along the propagation path.

Generally, most lasers are designed to operate in a fundamental Gaussian mode, which are always subjected to beam divergence as the beam waist becomes expanded at increasing distance. In a search for possible divergence-free laser beam, a new beam characteristic has to be considered. A strategy to overcome beam divergence should involve a non-vanishing radial wave component that propagates toward the beam center, in order to compensate the outward diffraction. It is known that a beam propagating through a conical lens or axicon pickups a radially propagating component simultaneous with the remaining axial wave propagation [7]. A beam generated by an axicon is generally described by a Bessel profile, which is ideally regarded as a non-diverging beam. Therefore, axicon system would be an interesting optic component, promising for practical generation of a long-distance collimated beam.

Furthermore, it has been reported that a Bessel beam has another intriguing property of self-reconstructive profile. That is, a laser intensity profile is well maintained as far as a Bessel beam propagates. If a Bessel beam encounters a fluctuating zone in a medium, the beam will be disturbed only for a short distance; then, the intensity profile will reconstruct itself and revert back into the original [8]. This makes a Bessel beam even more attractive for further investigation.

There are several methods that can be used to produce a Bessel beam, for instances, using circular slit followed by a Fourier transforming lens, or using an axicon lens. The latter method is proved to be very simple and convenient. A plano-concave axicon causes more divergent, while a plano-convex axicon converges the incident beam in a unique way, such that a small beam size is well confined along the axial direction rather than producing a tight focus as commonly obtained from a normal spherical lens.

Nevertheless, at current lens polishing technology, an angle tolerance is not small enough to produce an axicon with ultra-small base angle. As such, a single axicon is not capable of producing diffraction-free beam for a kilometer distance. Therefore, a compound axicons structure, analogous to a cemented doublet lens, with spacer layer filled with optical adhesive would be a simple but powerful strategy to generate Bessel-like beam with much longer propagating distance. However, the beam propagation characteristics of a compound axicon depends on several factors, involving axicon base angles, glass materials, input beam waist, and most importantly the refractive index of inter-axicon material, which are the subjects to be investigated in this project.

To perform numerical study, the finite element method (FEM) was applied to solve electromagnetic wave equation for investigating the transformation of an input Gaussian beam into a Bessel-like beam after propagating through an axicon doublet. Since the numerical calculation is intended for a km-long propagation domain, vast amount of mesh elements are required to obtain accurate result. This would be practically impossible to implement the particular investigation in conventional methods in wave optics modules. Therefore, the beam envelop method in COMSOL Multiphysics® was employed in this work, as the only slowly-varying detail of an envelope amplitude function is solved, which requires much lesser amount of computing resources.

2. Theory

In this simulation, an outgoing electromagnetic wave from a compound axicon is numerically solved upon an injection of a Gaussian beam as an incident wave. Considering time-harmonic field, the spatial evolution of an interested electromagnetic wave can be described by,

$$\mathbf{E}(\mathbf{r}) = \mathbf{E_1}(\mathbf{r})e^{-j\mathbf{k}.\mathbf{r}} + c.c., \tag{1}$$

where $\mathbf{E_1}$ is the envelope amplitude function, and the $e^{-j\mathbf{k}.\mathbf{r}}$ is a usual rapidly-varying phase factor. For a wave that propagates in *y*-direction through a lossless and nonmagnetic medium, the Maxwell's wave equation reads,

$$\left(\nabla_\perp + \frac{\partial}{\partial y}\hat{e}_y\right) \times \left(\nabla_\perp + \frac{\partial}{\partial y}\hat{e}_y\right) \times \mathbf{E} - k_0^2 n^2 \mathbf{E} = 0, \tag{2}$$

where $\nabla_\perp = \frac{\partial}{\partial x}\hat{e}_x + \frac{\partial}{\partial z}\hat{e}_z$ is the divergence operator in the transverse direction. In this work, the propagation of an electromagnetic wave needs to be solved in a very long computation domain, which is ~10^6-10^7 times larger than the optical wavelength. Since accurate numerical calculation prefers mesh size at least 10 times smaller than the wavelength, direct solve for the full wave equation above would require tremendous amount of memories. Therefore, by introducing an approximation that the envelop field amplitude $\mathbf{E_1}$ is slowly-varying along the propagation direction, i.e. $\left|\frac{\partial^2 \mathbf{E_1}}{\partial y^2}\right| \ll \left|\frac{\partial \mathbf{E_1}}{\partial y}\right|$, then we can decouple the rapidly-varying factor, e^{-jky}, from the wave equation (2) and arrive at the evolution equation for the envelope amplitude as,

$$i\frac{\partial \mathbf{E_1}}{\partial y} = \frac{1}{2k_0 n}\nabla_\perp^2 \mathbf{E_1}. \tag{3}$$

This requires the solver to solve only for the slowly-varying $\mathbf{E_1}$ variable, which permits the use of much bigger mesh size along the propagation direction.

2.1 Gaussian beam

A 2D Gaussian beam in fundamental mode was used as an incident beam for this simulation, and it was released at a matched boundary using the following beam definition,

$$E(x,y) = E_0 \frac{w_0}{w(y)} e^{-x^2/w^2} e^{-j\varphi}, \tag{4}$$

where $= ky - atan\frac{y}{z_R} + \frac{kx^2}{2R(y)}$, is called Gouy phase shift, $z_R = \frac{\pi {w_0}^2}{\lambda}$ is the Rayleigh range. Figure 1 shows the shape of a Gaussian beam along the *y*-axis propagation direction.

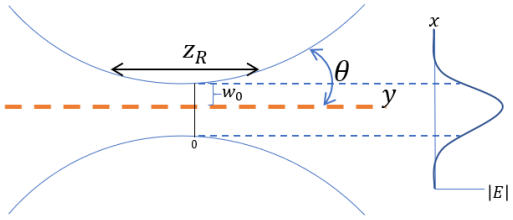

Figure 1 Description of a Gaussian beam

2.2 The normalization factor

The incident Gaussian beam is normalized to the laser input power using the following relationship between electromagnetic wave intensity and electric field as,

$$I = 2nc\varepsilon_0|E|^2. \tag{5}$$

For a laser beam travelling through an arbitrary cross-sectional area A at position *y*, the total beam power is $P = \iint IdA$, which results in a normalization factor as

$$E_0 = \sqrt{\frac{P}{nc\epsilon_0 \pi w_0^2}}. \quad (6)$$

Therefore, a power-normalized Gaussian beam can be expressed as,

$$E = \sqrt{\frac{P}{nc\epsilon_0 \pi w^2(y)}} e^{-x^2/w^2} e^{-j\varphi}, \quad (7)$$

2.3 Bessel beam

Although the aim of this work is to calculate numerically for a Bessel-like beam profile generated from a compound axicon, a brief mathematic description of a Bessel beam is also given. Considering for a cylindrically symmetric electromagnetic wave that propagates in *y* direction, the wave function takes the following form [9],

$$E(\mathbf{r}) = E(\rho)e^{-jk_y y}, \quad (8)$$

where $\rho = \sqrt{x^2 + z^2}$ and $E(\rho)$ represents a radial field component. The corresponding Maxwell's wave equation in cylindrical coordinate becomes,

$$\frac{d^2E}{d\rho^2} + \frac{1}{\rho}\frac{E}{d\rho} + (k^2 - k_y^2)E = 0. \quad (9)$$

The above equation is also a well-known form of Bessel differential equation. The zeroth-order solution for the radial waves takes the form of Bessel function of the first kind as,

$$E(\rho) = J_0(k_x \rho), \quad (10)$$

where ${k_x}^2 + k_y^2 = k^2$. Therefore, it exists a real parameter θ such that

$$k_x = k\sin\theta \text{ and } k_y = k\cos\theta, \quad (11)$$

which corresponds to a relative angle of *k* and k_y as illustrated in Figure 3. This diagram also indicates the radial wave component, k_x. Finally, the desired diffraction-free Bessel wave in 2D can be written as

$$E(x, y) = J_0(k_x \rho)e^{-jk_y y}, \quad (12)$$

2.4 Bessel-Gauss beam

In practice, a pure Bessel beam cannot be generated from an axicon, since the input beam is not a perfect plane wave, but rather a common Gaussian laser beam. Therefore, the output beam after passing through an axicon will be more accurately described by a Bessel-Gauss profile. This is actually a Gaussian profile modulation on a normal Bessel beam as described by the following expression,

$$E(x, y) = E_0 J_0(k_x x)e^{-x^2/w^2} e^{-j\varphi}. \quad (13)$$

The above Bessel-Gaussian profile inherits beam spreading characteristic form a Gaussian intensity distribution Still, the travelling length is much longer, owing to the presence of an inward beam component that slows down the diffraction.

3. Implementation COMSOL Multiphysics®

A conceptual diagram of waves and all optics components are presented in Figure 3. Here, a Bessel-Gauss beam is generated through a cemented aixcon doublet structure consisting of a plano-convex and plano-concave axicons with base angles denoted as γ_1 and γ_2 respectively. In the middle, a gap is filled with a thin layer of optical adhesive, whose refractive index can be tuned by a mixture of optical adhesives or synthetic polymers [10]. This inter-axicon layer plays a major role as it adds a flexible degree of freedom into the optical design, while the γ_1 and γ_2 here are somewhat more constrained by the market availability. A Gaussian beam is incident normally on one side of a compound axicon and the produced Bessel-Gauss beam is investigated for its intensity profile along the diffraction-free range, defined as y_{max}.

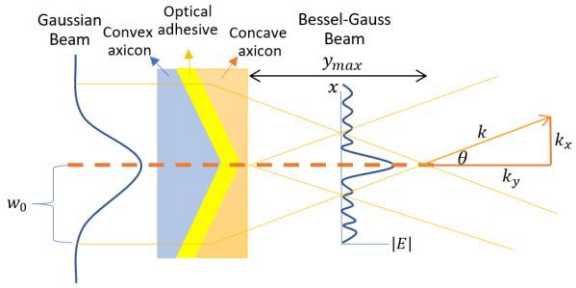

Figure 3 Bessel-Gauss beam generation from a compound axicon

For setting in COMSOL Multiphysics®, the Electromagnetic Wave Beam Envelop (ewbe) interface is chosen solve wave equation in a very large computation domain compared with optical wavelength. As the beams involved in this problem are all azimuthally symmetric, a 2D geometry is sufficient to study wave behaviors without loss of generality while keeping computation resources minimum. For the present model, a rectangular domain was built with

high aspect ratio, where the height is in few kilometers range while the width is in tens mm scale. The configuration of a compound axicon composes of a plano-concave axicon with $\gamma_2 = 0.5°$ stacking on a plano-convex axicon with $\gamma_1 = 1.0°$ as illustrated in Figure 4. All axicon thicknesses were set to 5 mm. The refractive indices $n_1 = 1.520$ and $n_2 = 1.461$ were assigned for a plano-convex and a plano-concave domain using the values from BK7 glass and fused silica, respectively, evaluated at a laser wavelength of 532 nm. The effect of interlayer index in a range of n_3 = [1.573, 1.580] was investigated through parameter sweeping.

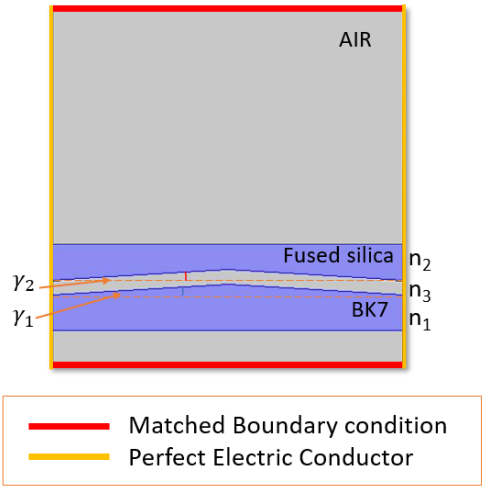

Figure 4 Geometry of a designed compound axicon placed with in a long propagation domain (not to scale)

In addition, a matched boundary condition was applied to the bottom boundary with an input Gaussian beam set to propagate in positive *y*-direction with waist diameter w_0= 25 mm. Another matched boundary with no wave excitation was set for the top boundary. Both side boundaries were set as perfect electric conducting condition, based on assumption that the wave energy drops rapidly in radial direction away from the beam center. Also, the wave vectors for each domain were calculated based on the Snell's law, and inserted properly in the module setting.

Mesh dimensions were designed differently to suite the propagation and transverse directions of the beam. Since the evolution of field amplitude is much slower in the *y* direction, we therefore decided to mesh the geometry using mapped structure with larger mesh size along the *y* axis, while denser mesh elements were designated for the *x* direction as shown in Figure 5.

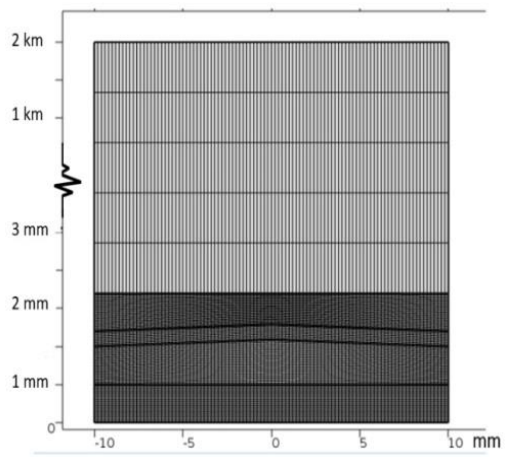

Figure 5 Meshing for an investigated geometry

4. Results and Discussions

It has been trialed and found that the compound axicon with the order, axicon angles, and axicon refractive indices given in previous section is one of the most effective configuration that result in a properly slow beam converging. Therefore, the only parameters left to investigate are the refractive index of the spacer layer, and the input beam waist diameter. Figure 6 shows the effect of n_3 on the axial intensity along the propagation distance for generated Bessel-Gauss beams with initial w_0 = 25 mm. Obviously, there exists an optimum value of the spacer refractive index, i.e. $n_3 = 1.577$, upon which the resulting beam intensity extends to the longest distance over 2 km with the final intensity nearly equals the initial value.

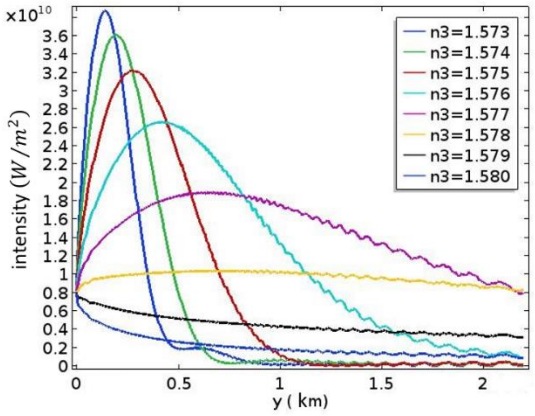

Figure 6 Effect of n_3 on longitudinal intensity of Bessel-Gauss beam with w_0 = 25 mm

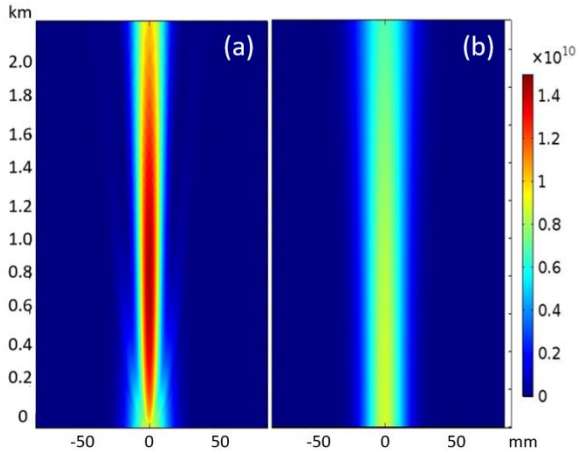

Figure 7 Comparison of intensity profile for (a) Bessel-Gauss and (b) Gaussians beams at waist diameter 25 mm

Also, smaller n_3 values are found to cause too much beam convergence, such that the intensity peaks very early nearer to the release position. Then the intensity drop quite sharply along the propagation distance. On the other hand, larger n_3 value leads to the beam divergence, which results in the unfavorably monotonic drop of laser intensity. Notably, it is found that the intensity profile of a generated Bessel-Gauss beam is relatively sensitive to the change of spacer index on the order of ~0.06%; therefore, other possible parameters that could affect the refractive index e.g. temperature, polarization or humidity should be accounted for further investigations.

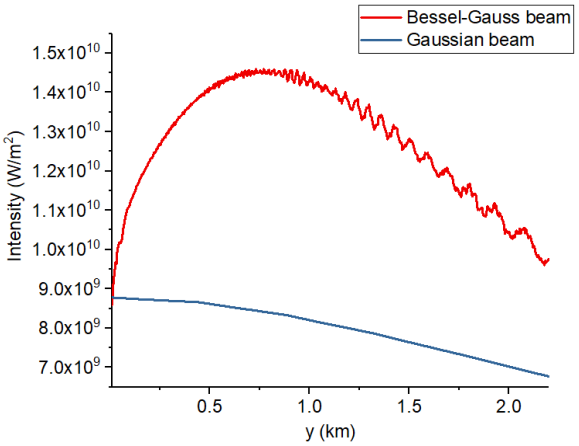

Figure 8 Longitudinal beam intensity for w_0 = 25 mm

At the optimal $n_3$value, the corresponding beam intensity distribution of the generated Bessel-Gauss beam is determined in comparison with a normal Gaussian beam with the same input waist diameter of 25 mm, shown in Figure 7. Clearly, the overall beam size of a Bessel-Gauss becomes smaller than an input Gaussian beam due to the right converging angle that keeps the axial collimation of the beam against the diffraction. This smaller beam size leads to higher beam intensity when compared to the diverging Gaussian beam. The longitudinal intensity distributions, displayed in Figure 8, also confirm superior power delivery to a long distance for the case of Bessel-Gauss beam. The intensity actually rises up during the middle range of the propagation before slowly reducing to the value close to the original intensity even at long distance. In contrast, Gaussian beam intensity only drops monotonically for the increasing distance.

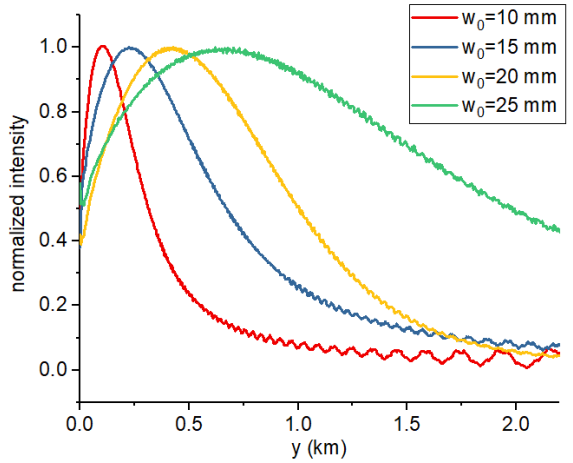

Figure 10 Effect of input beam waist on longitudinal beam intensity of a produced Bessel-Gauss beam

Beside the refractive index of spacer layer, the effect of input beam waist on the intensity evolution along the travelling distance is also investigated and the numerical result is displayed in Figure 10. In general, a larger input beam waist produces a Bessel-Gauss beam travelling longer before losing the power as the beam is beyond the diffraction-free range. This can be attributed to the longer overlapping range of the converging beam and also the lower diffraction rate of a modulated Gaussian beam

5. Conclusions

We performed simulation to investigate the generation of a Bessel-Gauss beam with divergence-free propagation range in kilometers scale. The beam was generated from a cemented axicon doublet with a Gaussian beam employed as an input. The finite element calculation in large domain was made possible using beam envelop method that reduces the number of mesh elements. The result is promising such that a well collimated beam of waist only 25 mm can be delivered over the distance at least 2 km.

6. References

[1]. J. Chance Carter, Standoff Detection of High Explosive Materials at 50 Meters in Ambient Light Conditions Using a Small Raman Instrument, *Applied Spectroscopy*, **Vol. 59**, pp.769-775 (2005)

[2]. Stephen E. Reutebuch, An Emerging Tool for Multiple Resource Inventory, *Journal of Forestry*, **Volume 103**, Pages 286–292 (2005)

[3]. Chein-I Chang, *Techniques for Spectral Detection and Classification*, Springer Science & Business Media (2003)

[4]. Peter M. Livingston, Laser anti-missile defense system, *Northrop Grumman Systems Corp*, (1993)

[5]. Jennifer C. Ricklin and Frederic M. Davidson, implications for free-space laser communication, *Journal of the Optical Society of America A*, **Vol. 19**, (2002)

[6]. Jones, L. W. and Keefer, D. R., NASA's laser-propulsion project, *Astronautics and Aeronautics*, **vol. 20**, p. 66-73 (1982)

[7]. Philip Birch, Long Distance Bessel Beam Propagation Through Kolmogorov Turbulence, *Journal of the Optical Society of America*, (2015)

[8]. Z. Bouchal, J. Wanner and M. Chlup, Self-reconstruction of distorted nondiffracting beam, *Optics Communications*, p. 207-211. (1998)

[9]. Kirk T. McDonald, Bessel Beams, *JosephHenry Laboratories Princeton University*, (2000).

[10]. Jin-Kyu Choi, Observation of Tunable Refractive Indices and Strong Intermolecular Interactions in Newly Synthesized Methylene-biphenylene-Bridged Silsesquioxane Thin Films, *the journal of physical chemistry***,** pp 14233-14239 (2010)

7. Acknowledgements

This work was funded by Development and Promotion of Science Technology Talents (DPST) Research Grant (Grant No. 0012559). We also would like to thanks the NanoPhotonics research group for continual supports.